Histol Histopathol (2014) 29: 1423-1435
DOI: 10.14670/HH-29.1423

http://www.hh.um.es

Histology and Histopathology
Cellular and Molecular Biology

Effect of prior exercise training and myocardial infarction-induced heart failure on the neuronal and glial densities and the GFAP-immunoreactivity in the posterodorsal medial amygdala of rats

Ana Paula S. Salazar[1], Edson Quagliotto[2], Jadson Alves[2], Fernando A. Oliveira[2], Lisiani Saur[3], Léder L. Xavier[3], Aline S. Pagnussat[1] and Alberto Rasia-Filho[1,2]

[1]PPG-CR, Federal University of Health Sciences of Porto Alegre, Brazil, [2]Laboratory of Physiology, Department of Basic Sciences, Federal University of Health Sciences of Porto Alegre, Brazil and [3]Laboratory of Cellular and Tissue Biology, Faculty of Biosciences, PUCRS, Porto Alegre, Brazil

Summary. Exercise training has neuroprotective effects whereas myocardial infarction (MI) and heart failure (HF) can cause neuronal death and reactive gliosis in the whole amygdala. The posterodorsal medial amygdala (MePD) is involved with cardiovascular reflexes and the central control of sympathetic/parasympathetic responses. Our aim was to study the effects of prior exercise training and of MI-induced HF on the neuronal and glial densities and the glial fibrillary acidic protein-immunoreactivity (GFAP-ir) in the MePD of adult male rats. Animals (n=5/group) were: control, sedentary submitted to a sham MI (Sed Sham), sedentary submitted to MI/HF (Sed HF), trained on a treadmill and submitted to a sham MI (T Sham) or trained on a treadmill and submitted to MI/HF (T HF). The number of neurons and glial cells in the MePD was estimated using the optical fractionator and the GFAP-ir was quantified by optical densitometry. In the respective groups, treadmill training improved physical performance and MI damaged near 40% of the left ventricle. There was a hemispheric lateralization effect on the density of neurons (higher in the right MePD), but no significant difference in either the neuronal or the glial densities due to experimental condition. Regional GFAP-ir results revealed that the Sed HF group had a higher expression in the left MePD compared to the control and the Sed Sham rats ($p<0.01$). The present data did not evidence the effects of training or MI/HF in the MePD cellular density, but indicate a possible local restructuring of astrocytic cytoskeleton after MI/HF in rats.

Key words: Extended amygdala, Optical fractionator, Cellular density, Astrocytic cytoskeleton

Offprint requests to: Prof. Alberto A. Rasia-Filho. Federal University of Health Sciences of Porto Alegre, Dept. Basic Sciences / Physiology, Sarmento Leite 245, Porto Alegre RS 90170-050, Brazil. e-mail: rasiafilho@yahoo.com or: aarf@ufcspa.edu.br

Introduction

The rat posterodorsal medial amygdala (MePD), a major component of the "extended amygdala" (de Olmos et al., 2004), is an important part of the neural network that modulates the occurrence of social/reproductive behaviors (Newman, 1999; Dall'Oglio et al., 2008; Rasia-Filho et al., 2012b) and stress responses (Marcuzzo et al., 2007; Singewald et al., 2008). The MePD also has connections with various amygdaloid and hypothalamic nuclei and brain stem areas (Canteras et al., 1995; Petrovich et al., 2001; Saha, 2005) that receive cardiovascular sensorial afferences and that can ultimately regulate the heart rate (HR) and arterial blood pressure (AP) (Turner et al., 1986; Longhurst, 2008) under common physiological conditions and in both adaptive or pathological circumstances (Kubo et al., 2004; Davern and Head, 2011; Quagliotto et al., 2012). The MePD alters the baroreceptor- and chemoreceptor-mediated reflexes and the concomitant central sympathetic and/or parasympathetic cardiovascular adjustments (Quagliotto et al., 2008, 2012; Neckel et al., 2012). For example, microinjections of the major neurotransmitters glutamate and GABA in the right MePD induced, respectively, selective activations of the

sympathetic and parasympathetic components of the baroreflex in awake rats (Neckel et al., 2012).

Physical exercise training protects the cardiovascular system by modulating the sympathetic and parasympathetic output to cardiac and vascular functions (Joyner and Green, 2009; Gielen et al., 2010) as well as improving the outcome of acute myocardial infarction (MI) (Freimann et al., 2005; Jorge et al., 2011). In addition, regular aerobic exercise or rearing in enriched environments allow the development of motor skills and increase cerebral blood flow (Swain et al., 2003; Eadie et al., 2005). Training experiences reorganize neural circuitries in the motor cerebral cortex (Adkins et al., 2006), induce dendritic restructuring and spine plastic changes in the dentate gyrus (Eadie et al., 2005) and cerebellar cortex (Gonzalez-Burgos et al., 2011), and enhance memory and learning in rodents (Wu et al., 2007; Liu et al., 2009; Stranahan et al., 2011). Physical activity prevents the damage and neuronal loss induced by excitotoxic agents (Carro et al., 2001). Physical activity of moderate intensity also has neuroprotective properties, as evidenced by the reduction in the ischemia-induced neuronal cell death in the dentate gyrus (Sim et al., 2005; Zheng et al., 2006; Scopel et al., 2006; Cechetti et al., 2007). On the other hand, MI is one of the most common causes of chronic heart failure (HF) and affects both central and peripheral organs. Notably, neuronal death can occur due to apoptosis in different brain regions after MI in rats (Kaloustian et al., 2008). That occurred in the whole amygdala 3 days after MI (Wann et al., 2006) or in the lateral and medial nuclei of the amygdala, in the hippocampal CA1 area, in the dentate gyrus (Wann et al., 2006; Kaloustian et al., 2008) and in some hypothalamic nuclei at 1, 2 and 7 days following MI (Kaloustian et al., 2008). Additionally, cell death and reactive gliosis were found in the whole amygdala 14 days after MI in rats (Bae et al., 2010), as evaluated by the expression of glial fibrillary acid protein (GFAP), a major component of the mature astrocytic cytoskeleton (Pekny and Pekna, 2004; Middeldorp and Hol, 2011).

These data are interesting because they indicate a structural remodeling of brain areas after MI and, more specifically, in different amygdaloid nuclei that have integrative roles in neuroendocrine secretion and behavioral display (Dayas et al., 1999; Rasia-Filho et al., 2000, 2012a; Marcuzzo et al., 2007). In this sense, the MePD has an evident role in the modulation of activities that require motor activation, such as sexual and aggressive behaviors (reviewed in Newman, 1999; Rasia-Filho et al., 2012a), as well as in ongoing cardiovascular adjustments (Quagliotto et al., 2012). However, it is not currently known whether prior exercise training or MI/HF can alter the number of neurons and glial cells or the astrocytic cytoskeleton in the MePD of rats. It is well described that aerobic training reduces the sympathetic tone at the same time that it increases the parasympathetic one (Martins-Pinge, 2011) whereas cases of HF with an over-activation of the sympathetic tone are directly related to greater disease severity and increased mortality rate (Martins-Pinge, 2011). Given its role in central cardiovascular control, the MePD is a putative candidate where both the neuroprotective effects of training (Eadie et al., 2005; Adkins et al., 2006; Scopel et al., 2006; Cechetti et al., 2007; González-Burgos et al., 2011) and the marked cellular loss following MI/HF would occur (Wann et al., 2006, Kaloustian et al., 2008; Bae et al., 2010). Here, we focused on the MePD, and not the whole amygdala, to avoid including other anatomically and functionally heterogeneous nuclei and subnuclei at the same time. Our aim was to test the effects of exercise training and MI-induced HF on the neuronal and glial densities and the GFAP-immunoreactivity (GFAP-ir) in the MePD of male rats. We also evaluated if the present experimental manipulation could result in hemispheric differences in the MePD, since previous reports showed laterality effects for the density of neurons and glia cells (Johnson et al., 2008; Morris et al., 2008) and the synaptic organization (Brusco et al., 2014) of this area in adult rats.

Materials and methods

Animals

Adult Wistar male rats (3 months-old and weighing 200-250 g) were obtained from a local facility (Federal University of Health Sciences of Porto Alegre, Brazil; UFCSPA) and kept in groups with food and water *ad libitum*. Room temperature was maintained at 22±1°C in a 12 h light:dark cycle (lights off at 7 p.m.). All efforts were made to minimize the number of animals and their suffering. Animals were manipulated according to international laws for ethical care and use ('European Convention for the Protection of Vertebrate Animals used for Experimental and other Scientific Purposes', Council of Europe No 123, Strasbourg 1985), conformed to national guidelines and was approved by the local Ethical Committee (UFCSPA protocol no. 053-11).

Twenty-five rats were randomly assigned to the following groups (n=5 each): (1) non-manipulated control (Cont), whose rats were not submitted to any undue stress or experimental procedure, (2) sedentary rats submitted to a sham MI procedure (Sed Sham), (3) sedentary rats submitted to the surgical occlusion of the left descending coronary artery to induce MI and subsequent development of HF (Sed HF), (4) exercise-trained rats submitted to a sham MI (T Sham), and (5) exercise-trained rats submitted to MI and subsequent HF (T HF). The experimental design is shown in Fig. 1 and described in detail below.

Preconditioning training protocol

Rats that composed the two trained groups (T Sham and T HF) were habituated to an adapted motorized rodent treadmill ("Athletic Racer", Brazil) during 1 week to minimize novelty stress. Animals that composed the groups of sham training (Sed Sham and Sed HF)

were set in the same experimental room and were placed on the treadmill turned off during the same time as the trained groups (20 min/day and 3 times/week), as described below.

Measurement of the maximum exercise test (ET) was realized in all animals of the trained groups both before the first day of training and in the middle of the exercise protocol. Each rat started running at a low treadmill speed with a pace increasing 5 m/min every 3 min. The point of exhaustion and the time to fatigue (in min) and workload (in m/min) were taken as indexes of capacity for exercise (Rodrigues et al., 2007). The exercise training intensity was set at 60% of the maximum speed of ET. Treadmill training lasted 20 min/day and was done 3 times/week during 4 weeks, based on (Real et al., 2013; Ben et al., 2009, 2010; Cechetti et al., 2007; Scopel et al., 2006).

Surgical procedure for myocardial infarction

Rats that composed the Sed HF and the THF groups were anesthetized with intraperitoneal injections of xylazine (12 mg/kg) and ketamine (90 mg/kg), intubated and artificially ventilated (SamWay VR 15, USA) to maintain a respiratory frequency of 60 breaths/min and an oxygen-inspired fraction of 100%. The MI was induced as previously described (Pfeffer et al., 1979; Jaenisch et al., 2011). Briefly, the heart was exposed through a left thoracotomy between the fourth and fifth ribs and a mononylon 6-0 suture closed the main left descending coronary artery between 1 and 2 mm distal to the edge of the left atrium. After that, the thoracic chest was closed, skin was sutured, the pneumothorax was drained by a continuous aspiration system, and animals received ibuprofen (oral administration of 100 mg/0.1 mL every 8 hours during the first postoperative day). The animals that composed the respective sham groups (Sed Sham and T Sham) underwent the same anesthetical and surgical procedure of heart manipulation, but no coronary manipulation.

We did not directly measure the final diastolic intraventricular pressure in those rats submitted to MI to avoid brain ischemic events that could affect cellular counts in the MePD and lead to misleading results. In another set of experiments, it was clearly observed that rats that underwent the same MI procedure as performed here (with similar left ventricle myocardial infarted areas) have a remarkable development of HF (Vanoli et al., 2004). Indeed, values of MI area higher than 25% and, more evidently, equal or higher than 40% highly correlates with the development of HF (Kclocke et al., 2007; Jaenisch et al., 2011; Tucci, 2011). Our present procedure led to mean MI areas of 39% in the left ventricle (see Results and Fig. 2B).

Stereological study

Experiments ended after 9 weeks (Fig. 1). That is, 4 weeks for the preconditioning training and 5 weeks following the MI induction as well as the respective sham procedures. Then, animals were deeply anesthetized with xylazine (12 mg/kg ip) and ketamine (90 mg/kg ip) and transcardially perfused with 0.9% saline (150 mL) and heparine (1200 IU/Kg) followed by 4% paraformaldehyde (PFA) in 0.1M phosphate buffer, pH 7.4% (150 mL). After perfusion, the hearts were removed and weighed. For those rats submitted to MI, left ventricles were filled with an insufflating latex balloon and placed in buffered formaldehyde for 24 h for subsequent analysis of the size of the infarction area (Fig. 2). The total left ventricle area and the myocardial infarction scar area were manually drawn on the scanned images and measured automatically using a computer program (Image Pro Plus 6.1, Media Cybernetics, USA). The infarction size is expressed as a percentage of the total left ventricle area (Pfeffer et al., 1979; Jaenisch et al., 2011).

Brains were removed, kept in 4% PFA for 24h, immersed in 15% and 30% sucrose solutions, frozen in isopentane and dry ice and maintained at -80ºC until further processing. Brains were sectioned using a cryostat (Leica, Germany) and each alternate serial coronal section of 30 μm-thick was stained with thionin for the stereological study or processed for the GFAP immunohistochemistry, as described below. All experimental groups were submitted to the same histological procedures and data collection. The rostro-caudal location of the MePD in the rat brain was based on the description provided by de Olmos et al. (2004) and compared with the schematic images of a rat brain atlas (Paxinos and Watson, 2005). The MePD was located laterally to the optic tract (OT) and ventrally to the stria terminalis (ST) in the rat ventral forebrain (Fig. 3). Although being continuous areas, the cyto-architectonical organization of the rostral and the caudal MePD appeared distinct (de Olmos et al., 2004). The rostral aspect of the MePD was arbitrarily set at 2.64 to 2.76 mm posterior to the bregma and the caudal aspect was at 3.36 to 3.48 mm posterior to the bregma (based on Paxinos and Watson, 2005). An evident medial column of cells was found in the MePD near the "molecular layer", a cell-sparse rim close to the OT (de Olmos et al., 2004; de Castilhos et al., 2006; Fig. 3). Both right and left hemispheres were studied separately and we tested for lateralized effects in the cellular components of the MePD (based on Johnson et al., 2008; Morris et al., 2008).

Thionin staining was done as reported elsewhere (Dall'Oglio et al., 2013). Briefly, brain sections were dried at room temperature (RT), immersed in different solutions of ethanol, cleared in xylene, immersed in a solution of 0.25% thionin for 3 min, immersed again in solutions of increasing ethanol concentration, dipped in a solution of 95% ethanol with 1% acetic acid and absolute xylene and were finally covered with synthetic balsam and coverslips.

For the stereological estimation, images were obtained with an Olympus BX61 microscope (400x,

Olympus, Japan) attached to a high-resolution digital D172 camera and a computer with the Image Pro Plus software. The neurons in the MePD were identified morphologically by their large, pale nuclei with an evident nucleolus and by the dark cytoplasm that contained Nissl bodies. The glial cells were identified according to their relatively small size and unstained cytoplasm. That is, the nucleolus was used as the counting marker for neurons, and the nucleus was used as the counting marker for glial cells (Fig. 3). No precise borders for the rostral, lateral and ventral limits of the MePD could be established along the whole extension of this subnucleus (see also the different editions of the atlas of Paxinos and Watson and other available atlases of the rat brain). A critical evaluation about this technical restriction was elaborated by us for both the rat and the human medial amygdala (Rasia-Filho et al., 2002; Dall'Oglio et al., 2013). Therefore, to avoid imprecise data collection and misleading results, cells were counted in the MePD medial cellular column taking the unequivocal presence of OT and the ST as anatomical references for all animals in all experimental groups.

The MePD cellular density (the number of neurons and glial cells) was estimated by the optical fractionator method. Five rats were studied in each experimental group. From each brain, 1 of 5 serial sections containing the MePD was selected proceeding along the rostro-caudal axis. From a total of 8-10 sections obtained per rat, we studied 3 sections in the rostral aspect and 3 in the caudal aspect of the MePD. Four squared counting frames [called the area of interest (AOI) with 1,203 μm^2] were randomly overlaid onto the medial column of the MePD in each studied section. The cells were counted at different focal planes, including the z axis, throughout the brain slice. Neurons and glia cells overlaying the "including" borders of the counting frame were counted as well as the cells located within the counting frame. Conversely, the cells overlaying the "excluding" borders of the counting frame were not counted (Dall'Oglio et al., 2013; Fig. 3).

The numerical density of neurons and glial cells was estimated using the following formula:

$Nv=(1/[a/f.h]) . (\Sigma Q/\Sigma P)$

Where, Nv=estimated numerical density, a/f=area of the counting frame; h=disector height; ΣQ=sum of cells counted and ΣP=sum of analyzed counting frames. The post-processing thickness of each brain slice was measured, and the section height was used as the disector height (Costa Ferro et al., 2010; Dall'Oglio et al., 2013).

From these data the neuronal/glial ratio was calculated by dividing the number of neurons per glial cells in the rostral and caudal MePD of each hemisphere and in each experimental group.

GFAP Immunohistochemistry and quantification

The procedure for GFAP immunohistochemistry was adapted from previous reports (Rasia-Filho et al., 2002; Martinez et al., 2006; Johnson et al., 2008). Briefly, the brain sections were mounted on histological slides, washed and then blocked with 2% bovine serum albumin (BSA) in PBS containing 0.4% Triton X-100 (PBS-Tx, Sigma Chemical Co., USA) for 30 min, and incubated with polyclonal GFAP antiserum raised in rabbit (Dako, UK) diluted 1:500 in 0.3% of PBS-Tx for 48 h at 4°C. After being washed with PBS-Tx twice, sections were incubated in anti-rabbit IgG peroxidase-conjugated antibody produced in goat (Sigma, USA) diluted 1:150 in PBS-Tx at RT for 2 h. The reaction was developed by incubating the sections in a medium containing 0.06% 3,3'-diaminobenzidine (DAB, Sigma Chemical Co., USA) dissolved in PBS for 10 min and in the same solution containing 1 μL of 3% H_2O_2 per mL of DAB medium for 10 min. Sections were rinsed again in PBS, dehydrated in a series of increasing ethanol concentrations (70, 90 and 100%, 2 min each) cleared with xylene and covered with Permount and coverslips. To control for non-specific binding, the primary antibody was omitted and replaced by PBS. No staining was evident after that. Furthermore, in order to minimize differences in the staining of astrocytes and in background levels, the brains in both experimental groups were fixed and post-fixed in identical solutions for the same length of time, processed at the same time and incubated in the same immunostaining medium for the same period of time (Saur et al., 2014). As a rule, GFAP-ir appeared similarly as found in other reports (Rasia-Filho et al., 2002; Dall'Oglio et al., 2013).

The intensity of GFAP-ir was measured using semi-quantitative densitometric analysis (Ferraz et al., 2003; Xavier et al., 2005; Martinez et al., 2006) using a BX 50 microscope (200x; Olympus, Japan) coupled to a Motic Images Plus 2.0 camera and Image Pro Plus software. One of 5 serial sections containing the rostro-caudal axis of the MePD was selected and converted to an 8-bit gray scale (256 gray levels). Five animals were studied in each experimental group (except the Cont and Sed Sham HF groups, where n=4), 5 sections were studied per rat (2 sections in the rostral aspect and 2 in the caudal aspect of the MePD). This same procedure was done for the right and the left hemispheres. Three AOIs (8,260 μm^2 each) were randomly overlaid on each section. These images were used in the analysis of regional optical density (OD; Saur et al., 2014). For the analysis of cellular OD, one AOI measuring 4.19 μm^2 was placed over the astrocytic soma in each studied image. The regional and the cellular ODs were calculated according to the following formula (Martinez et al., 2006):

$OD\ (x,y)=-\log [(INT_{(x;y)} - BL)]/(INC - BL)$

Where, OD(x,y) is the optical density at pixel (x,y), INT(x,y) is the intensity at pixel(x,y), BL or black is the intensity generated when no light goes through the material and INC" or incident is the intensity of the incident light. All lighting conditions and magnifications were kept constant during the process of capturing the images. Blood vessels and other artifacts were avoided and the background correction was performed according to the procedure previously described in Xavier et al. (2005).

Additional morphological analysis of GFAP-ir astrocytes was done using the same images employed to measure cellular OD. Three parameters were evaluated: (1) An adaptation of Sholl's concentric circles technique was used for the study of astrocytic ramification (Sholl, 1953; Saur et al., 2014). That is, 7 virtual concentric circles with 50 μm intervals were drawn around each astrocytic cell body. The degree of ramification of each astrocyte was measured by counting the number of times astrocytic processes intersected each virtual circle in both the lateral (i.e. right/left) and central (i.e. superior/inferior) quadrants around the astrocytes. (2) The quantification of primary processes was performed by directly counting the number of astrocytic prolongments extending from the soma in both the lateral and central quadrants. (3) The longest primary process in each quadrant was measured by tracing the process with a manual measurement tool found in the Image Pro Plus software (Saur et al., 2014).

Statistical analysis

The effectiveness of the training protocol was compared within-group (pre- and post-training performance) and between trained groups using a two-way analysis of variance (ANOVA) test for repeated measures. The infarcted area of the left ventricle was compared between HF groups using the two-tailed Fisher test. The density of neurons and glial cells, the neuronal/glia ratio and the different GFAP-ir parameters were compared in each hemisphere and location in the MePD (rostral and caudal aspects) among the experimental groups using an ANOVA test for repeated measures (considering the data from the right and left hemispheres) followed by the Tukey test or the Bonferroni test. The significant statistical level was set at $p \leq 0.05$.

Results

Training effect and infarction area

The exercise protocol was able to enhance the performance of trained rats (Fig. 2A). That is, the statistical analysis revealed that time spent exercising increased significantly [$F(1,7)=7.25$; $p=0.03$] and speed on the treadmill showed a clear trend to be improved [$F(1,7)=4.58$; $p=0.06$] when comparing the pre-training vs the post-training performance in the T Sham and the T HF groups. There was no interaction between training protocol and the rat experimental condition [$F(1,7)=0.03$; $p=0.85$ for the time spent on the treadmill; and, $F(1,7)=0.77$; $p=0.4$ for speed on the treadmill].

The left ventricular infarction area in the Sed HF and T HF groups did not show a statistically significant difference between groups (mean ± SD=40±7 and 38±6%, respectively; $p=0.8$; Fig. 2B).

Neuronal and glial densities in the right and left MePD

According to the aforementioned including criteria, the thionin staining allowed the identification of MePD neurons with round, fusiform or multiangular cell body shapes and the neuronal nucleus with an evident and single nucleolus. Glial cells had a comparatively small size, no nucleolus and an unstained cytoplasm (Fig. 3).

The density of neurons in the MePD showed a statistically significant difference due to hemispheric lateralization [$F(1,18)=56.54$; $p<0.01$; higher values in the right MePD, Fig. 4A], but there were no differences due to the group experimental condition [$F(4,18)=2.22$; $p=0.1$] or the interaction of these two factors, i.e., MePD laterality and experimental condition [$F(4,18)=2.25$; $p=0.1$; Fig. 4B,C].

The density of glial cells in the MePD showed no statistically significant difference due to hemispheric laterality [$F(1,18)=0.22$; $p=0.64$], experimental condition [$F(4,18)=2.31$; $p=0.1$] or the interaction of laterality and experimental condition [$F(4,18)=0.43$; $p=0.1$; Fig. 5A-C].

Likewise, there was no statistically significant difference among groups for the density of neurons and glial cells either in the rostral or in the caudal parts of the MePD ($p>0.05$ in all cases; Figs. 4B,C, 5B,C).

Calculated from the values shown in Figs. 4B,C, 5B,C, the neuronal/glia ratio varied among groups from 1.2 to 6.4 and 1.1 to 7.6 in the rostral and in the caudal MePD, respectively. In the rostral MePD there was a

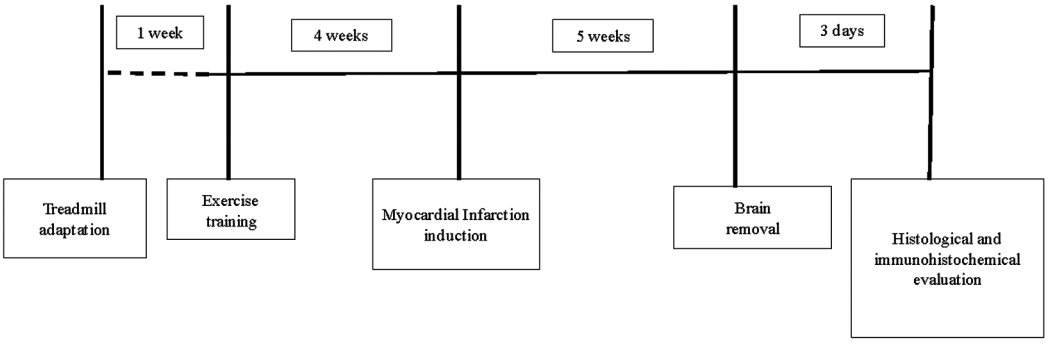

Fig. 1. Experimental design (in weeks and days) involving the preconditioning training and the myocardial infarction. Control animals were not manipulated whereas other control groups were submitted to "sham" procedures during this period. Further details are provided in the text.

statistically significant difference in the neuronal/glial ratio due to hemispheric laterality [F(1,20)=17.80; p<0.01; higher values in the right MePD], but no statistically significant difference due to experimental condition [F(4,20)=0.19; p=0.93] or the interaction of laterality and experimental condition [F(4,20)=0.72; p=0.58]. The same was found in the caudal MePD. That is, there was a statistically significant difference in the neuronal/glial ratio due to hemispheric laterality [F(1,20)=10.68; p<0.01; higher values in the right MePD], but no statistically significant difference due to experimental condition [F(4,20)=1.13; p=0.36] or the interaction of laterality and experimental condition [F(4,20)=0.13; p=0.96].

GFAP expression in the MePD

GFAP expression was found in the MePD of all experimental groups. Immunoreactive astrocytes were found isolated or in small clusters, with evident cell bodies and various branched prolongments (Fig. 6A).

The regional GFAP-ir in the MePD showed a statistically significant interaction for hemispheric laterality and experimental condition [F(4,16)=4.38; p=0.01; main differences in the left MePD]. That is, the Sed HF group showed an increased GFAP expression in the left MePD compared to the control and the Sed Sham data (p<0.01 in both cases). T Sham and T HF results were also higher than the control group (p<0.05 in both cases), but did not differ between them (p>0.05; Fig. 6B).

No statistically significant differences among experimental groups were found in the morphological features of the GFAP-immunoreactive astrocytes (ramification evaluated by the Sholl's concentric circles technique, number of primary processes or length of the

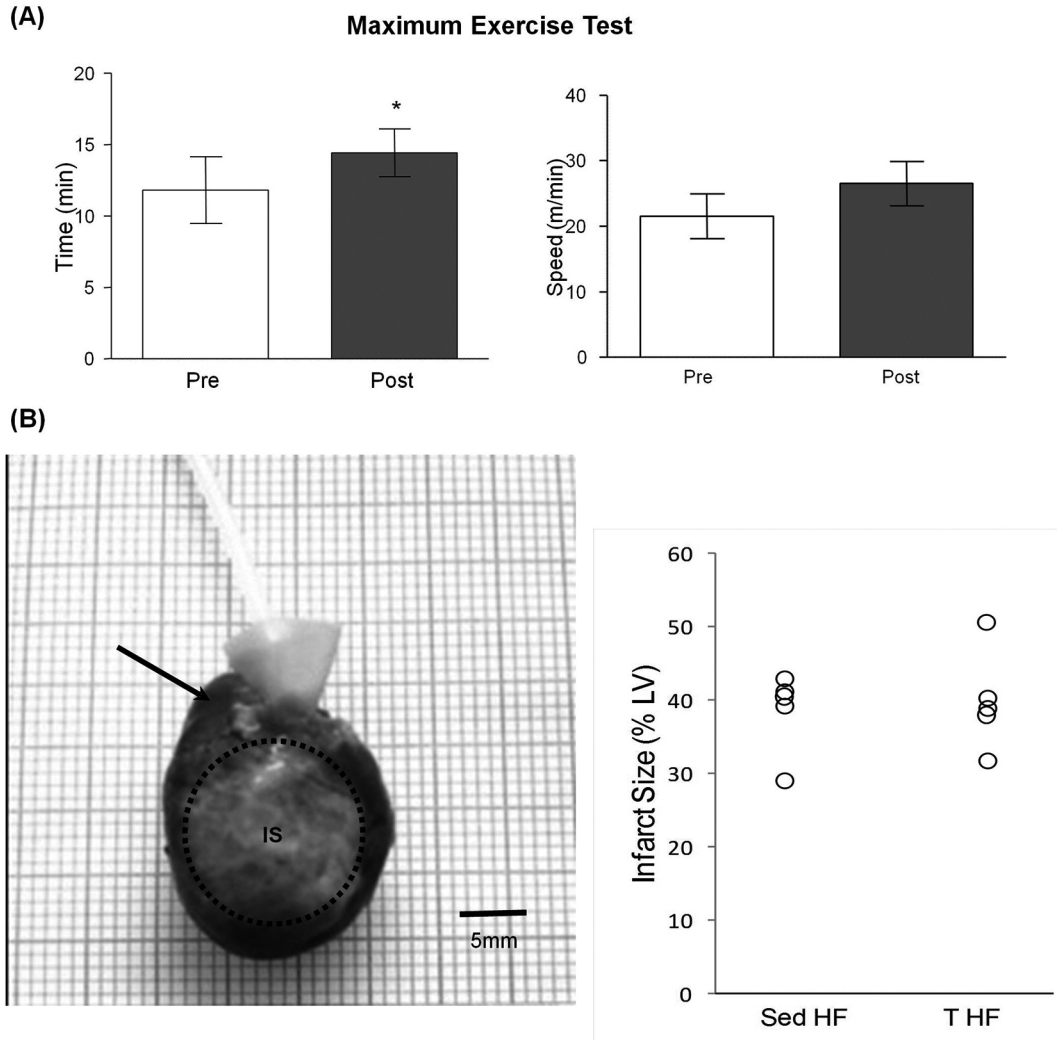

Fig. 2. A. Training effects, as evaluated by the maximum exercise test, on the time spent and on the speed on the treadmill of the aerobically trained rats submitted to a sham procedure or an effective myocardial infarction/heart failure (MI/HF). * p<0.05 compared to pre-training values. **B.** Left: Representative left ventricle frontal view as found in rats after 5 weeks of myocardial infarction. An insufflating latex balloon inside the ventricle allows the visual identification of the infarcted area (dashed lines). IS=Infarct size; in this representative case, approximately 40% of the left ventricle wall. The arrow points to the approximate location of the suture of the left coronary artery. Right: Summary plot of the infarcted area, as a percentage of the left ventricle wall, calculated for two experimental groups: sedentary rats submitted to the surgical occlusion of the left coronary artery and effective MI/HF (Sed HF) and exercise-trained rats submitted to MI/HF (T HF, n=5 rats/group).

primary processes; $p > 0.05$ in all cases, data not shown).

Discussion

The present results based on stereological and immunohistochemical approaches did not evidence a modification in neuronal or glial density in the MePD after exercise training and/or following MI/HF, but indicated a likely restructuring in GFAP-ir and astrocytic cytoskeleton after MI/HF in rats. Because the MI/HF condition did not affect relevant astrocytic morphological parameters, such changes found in the GFAP-ir could represent a redistribution of intermediate filaments in the already existing astrocytic branches extending within the MePD. This finding was previously linked with reactive gliosis after MI in the amygdala (Bae et al., 2010). These novel data add to the discussion of methodological differences in the evaluation of nervous tissue adaptation to physical exercise and to MI/HF and suggest the existence of different site-specific effects among brain areas involved in the elaboration of goal-oriented motor activity and the central control of cardiovascular responses, such as the rat MePD.

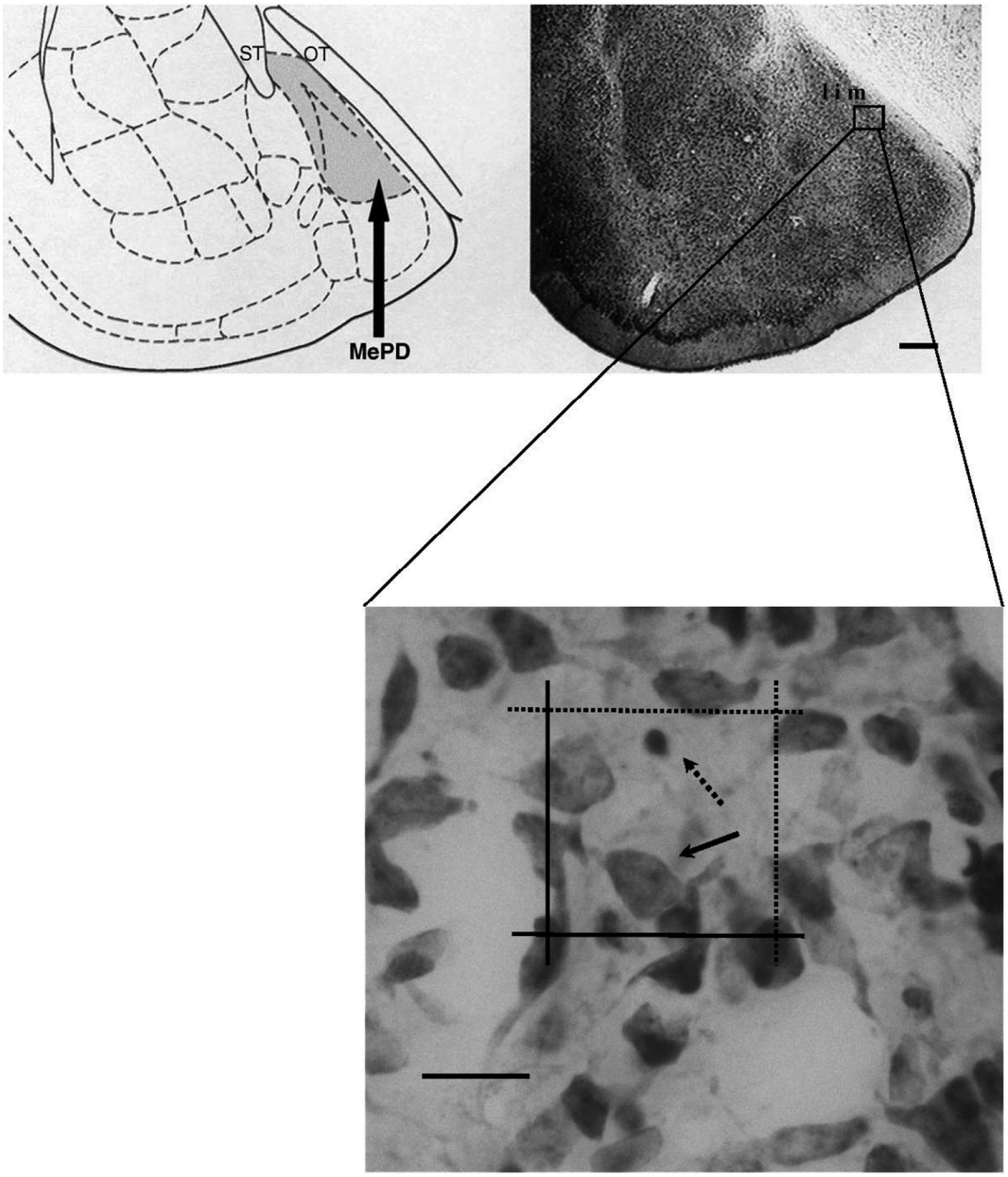

Fig. 3. Top, **Left panel.** Schematic diagram of a coronal brain slice showing the posterodorsal medial amygdala (MePD) in the ventral forebrain of rats, in this example at 3.14 mm posterior to the bregma. Adapted from Paxinos and Watson (1995). Top, **Right panel.** Histological staining used for the identification of the MePD in a matched coronally sliced brain section. The MePD was divided in medial (m), intermediate (i), and lateral (l) cellular columns. Stereological data was obtained from the medial column as illustrated. ST, stria terminalis; OT, optic tract. Scale bar: 300 μm. Reprinted from de Castilhos J., Marcuzzo S., Forti C.D., Frey R.M., Stein D., Achaval M., Rasia-Filho A.A. "Further studies on the rat posterodorsal medial amygdala: Dendritic spine density and effect of 8-OH-DPAT microinjection on male sexual behavior". Brain Res. Bull. 69, 131-139. Copyright (2008) with permission from Elsevier. **Bottom.** Photomicrographs of thionin-stained cells in the rat MePD at the magnification used for the optical fractionator stereological technique. The overlaid square represents the "area of interest" (1205 μm^2), where cells were counted, with including (solid lines) and excluding (dashed lines) borders. Example areas shown for a neuron (solid arrow) and a glial cell (dashed arrow). Contrast and background were adjusted using Photoshop 7.0, Adobe (USA). Scale bar: 25 μm.

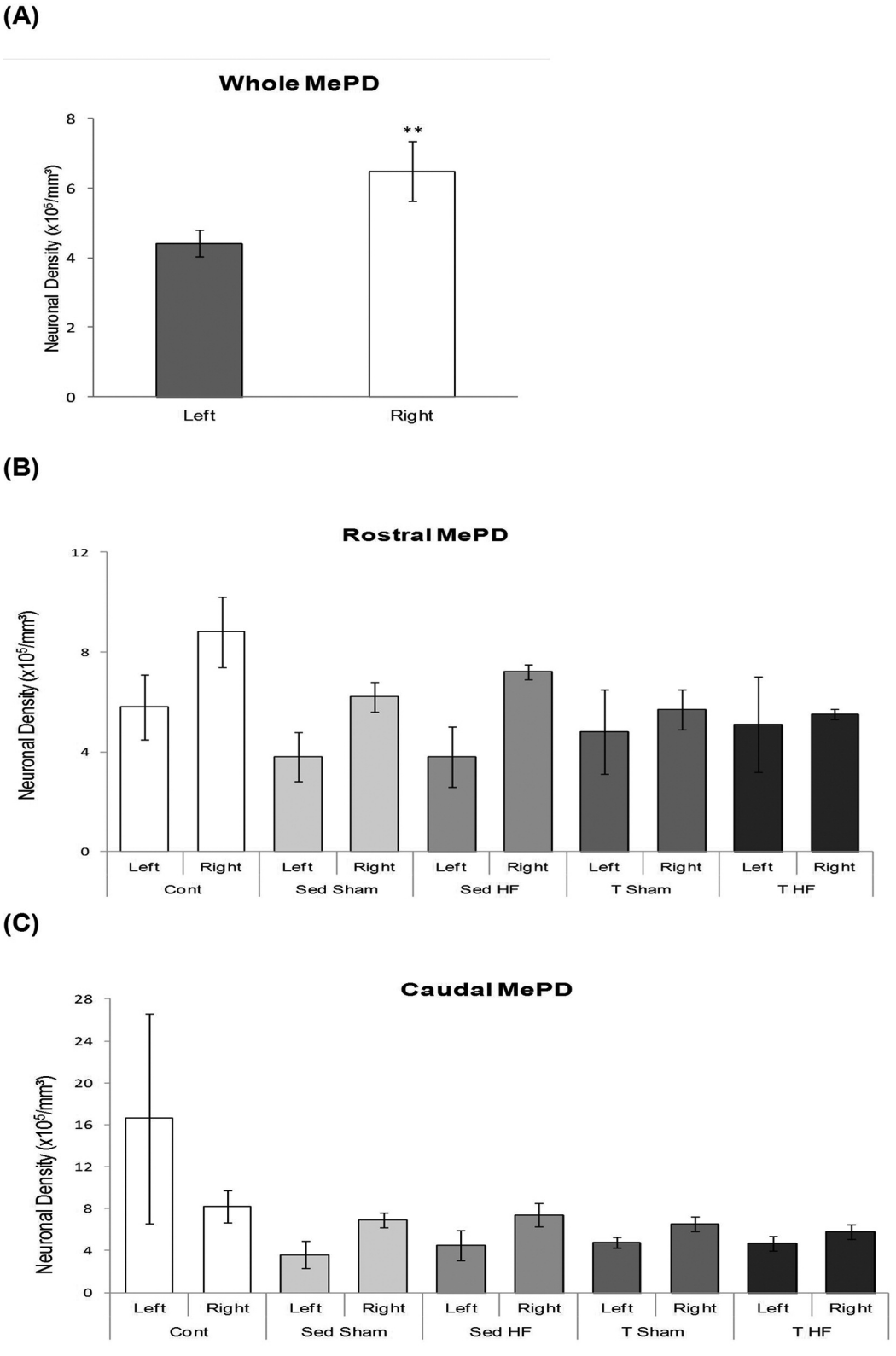

Fig. 4. A. Values are mean (± SD) of the stereological estimation of neuronal density and hemispheric difference found in the whole posterodorsal medial amygdala (MePD) of rats. **: $p<0.01$ compared to the left MePD. **B, C.** Mean (± SD) of the stereological estimation of the neuronal density found in the rostral **(B)** and caudal **(C)** aspects of the MePD and from the right and left hemispheres of non-manipulated controls, sedentary rats submitted to a sham MI (Sed Sham), sedentary rats submitted to the surgical occlusion of the left coronary artery and effective MI/HF (Sed HF), exercise-trained rats submitted to a sham MI (T Sham) and (5) exercise-trained rats submitted to MI/HF (T HF). Higher values were found in the right MePD compared to the left MePD but there were no statistically significant differences among experimental groups.

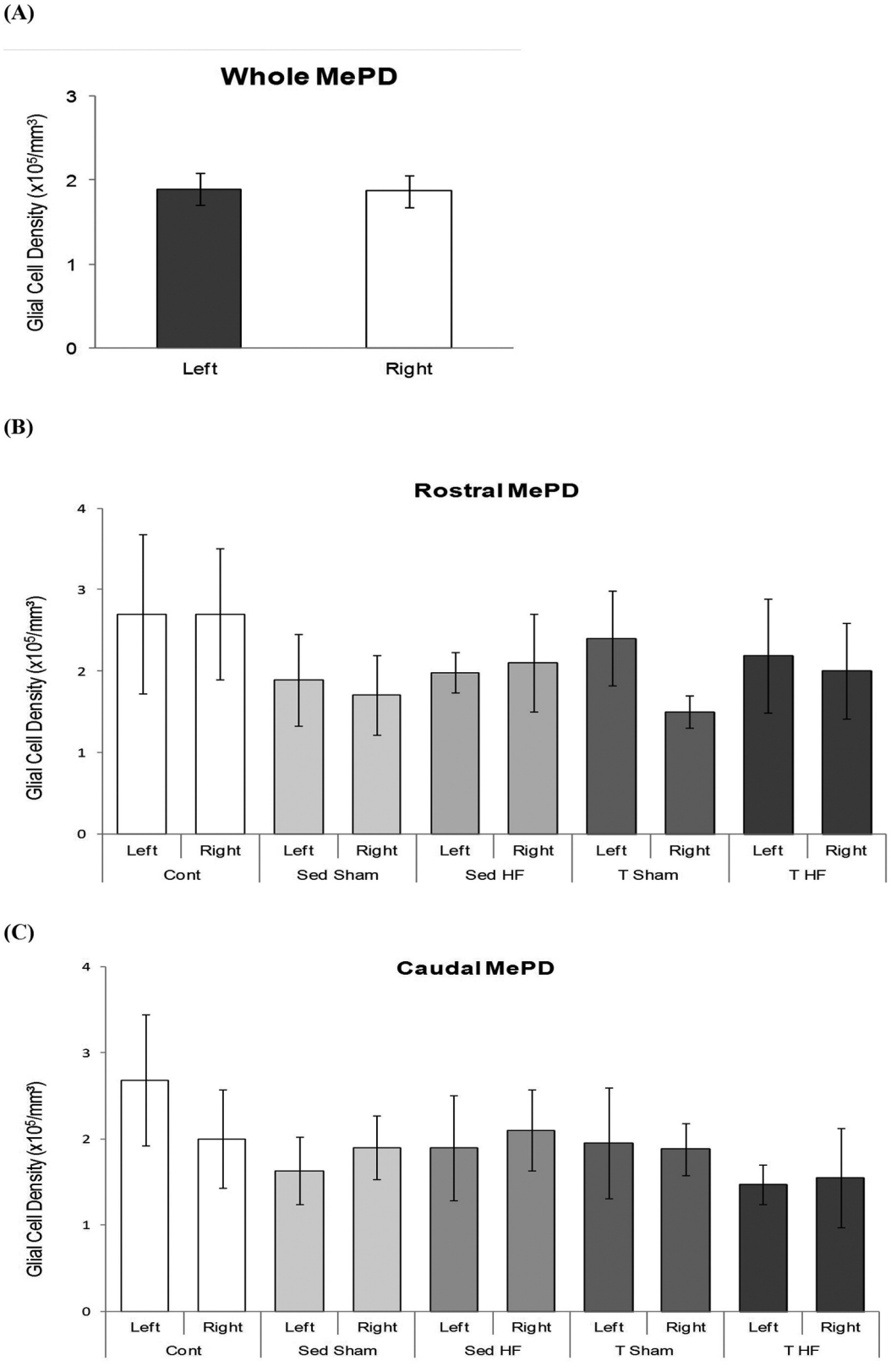

Fig. 5. A. Values are mean (± SD) of the stereological estimation of the glial density found in whole posterodorsal medial amygdala (MePD) of rats. **B, C.** Mean (± SD) of the stereological estimation of the glial cells density found in the rostral **(B)** and caudal **(C)** aspects of the MePD and from the right and left hemispheres of non-manipulated controls, sedentary rats submitted to a sham MI (Sed Sham), sedentary rats submitted to the surgical occlusion of the left coronary artery and effective MI/HF (Sed HF), exercise-trained rats submitted to a sham MI (T Sham) and (5) exercise-trained rats submitted to MI/HF (T HF). No statistically significant differences were found.

Here, we studied the medially densely-packed column of cells in the MePD to count neurons and glial cells because it was the place where effective neurotransmitters/neuropeptides microinjections initially reached and diffused into the MePD to modify the central cardiovascular control of HR and AP and to induce sympathetic/parasympathetic output changes (Quagliotto et al., 2008; Neckel et al., 2012). This MePD column of cells also showed notable Fos immunoreactivity following stressful stimulation and concomitant increases in HR and AP (Davern et al., 2010; Porter and Hayward, 2011). Taking these data into account, we tested the occurrence of plastic responses in this part of the MePD under the present experimental design. Both exercise training and MI were effective procedures. That is, training improved the performance of the animals in the treadmill protocol through 4 weeks of exercising, whereas the induced MI promoted a mean left ventricle infarcted area correlated with the development of characteristically impaired cardiovascular parameters of HF (Jaenisch et al., 2011).

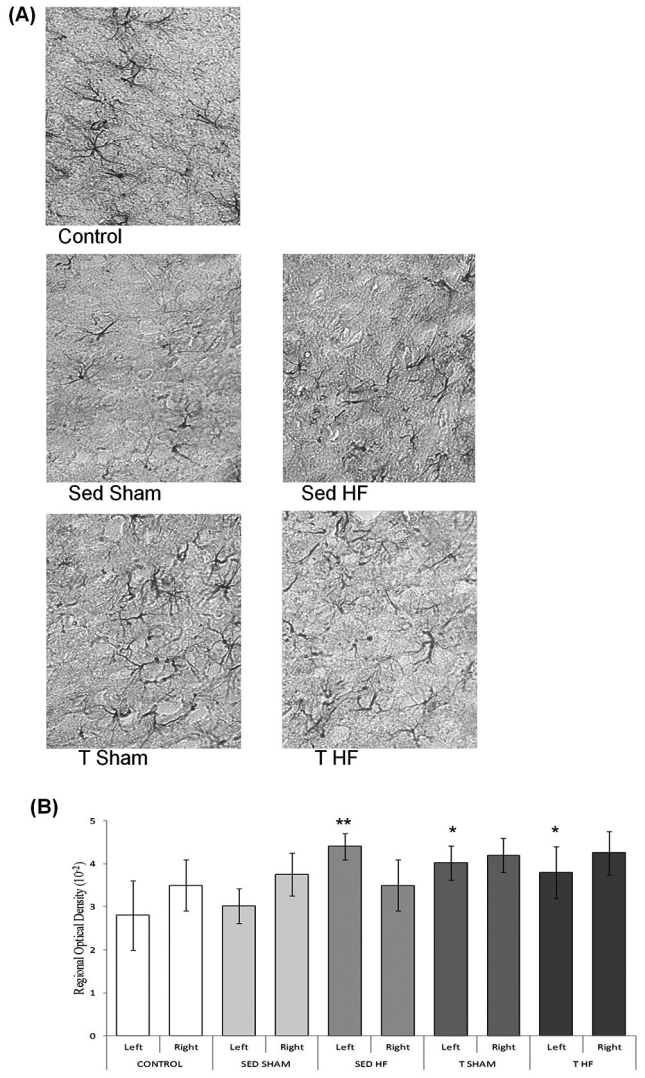

Fig. 6. A. Photomicrographs of the GFAP-immunoreactivity (GFAP-ir) pattern in the rat posterodorsal medial amygdala of non-manipulated controls, sedentary rats submitted to a sham MI (Sed Sham), sedentary rats submitted to the surgical occlusion of the left coronary artery and effective MI/HF (Sed HF), exercise-trained rats submitted to a sham MI (T Sham) and (5) exercise-trained rats submitted to MI/HF (T HF). Note the presence of astrocytic cell bodies and prolongments in all experimental groups, but apparently fewer cells in the Sed Sham and Sed HF groups. Contrast and background were adjusted using Photoshop 7.0, Adobe (USA). Scale bar: 50 μm. **B.** Values are mean (± SD) of regional optical density measurements of GFAP-ir in these same experimental groups. *: $p<0.05$ when compared to the control group data in the left hemisphere; **: $p<0.01$ compared to the Sed Sham data in the left hemisphere.

Although the experimental condition of the rats did not affect the density of neurons in the MePD, an inherent hemispheric lateralization difference was found in this morphological parameter. That is, the right MePD contains more neurons in its medial column of cells than in its left counterpart. Previous works have also shown a hemispheric specialization in neuronal number in the rat MePD (Morris et al., 2008) and compared adult male and female Long-Evans rats using the stereological optical fractionator method to count the number of cells. Higher values were found in males, independently of circulating androgens in these animals, and in both males and females there were more neurons in the left MePD (Morris et al., 2008). In our hands, the MePD of Wistar rats imposes difficulties for the exact delimitation of its borders (as described in "Stereological Study" above). Without consistency in this crucial condition, the Cavalieri method to estimate total number of cells can not be used. So, as a precaution to avoid potential confusion and unreal results (see a critical discussion in the preface of the rat brain atlas of Kruger et al., 1995), we decided to estimate the neuronal and glial densities in a part of the MePD that could be reliably found in all experimental groups. Here, Wistar rats showed another lateralized condition for the number of neurons in the MePD (i.e, higher values in the right hemisphere) and this might mean that more subtle subregion-specific differences can be found in this structure. It also has to be mentioned that rat strain differences were already reported for the whole medial amygdala, either for morphological data or for subcellular components and responses in local neurons (reviewed in Rasia-Filho et al., 2012b and references therein).

In this same regard, other authors used GFAP immunocytochemistry and found that the right MePD contains more astrocytes than the left MePD in Long Evans adult male rats (Johnson et al., 2008). Here we did not find a hemispheric specialization in the number of glial cells in the medial column of the MePD of Wistar rats among the studied groups, although regional GFAP-ir differences were found in the left MePD of the Sed HF group compared to the control data. Altogether, these findings point to a more complex condition of glial

presence and GFAP expression in the MePD of rats of different strains. Taking into consideration the methodological concerns that involve the specific epitope immunodetection in fixed tissue, it is also possible that direct comparisons of different immunohistochemical studies can be indeed controversial and it would be more appropriate to compare data "within" each experimental set.

We did not evidence a higher number of glial cells in the MePD suggestive of a proliferation of these cells after MI/HF. On the other hand, the higher GFAP-ir observed in the Sed HF group would represent a form of reactive gliosis with an increase in intermediate filaments after injury (Pekny and Pekna, 2004; Bae et al., 2010; Middeldorp and Hol, 2011), but not in the number and length of primary processes or the number of prolongments crossing the Sholl concentric circles around the cell body. Other authors have also shown higher GFAP-ir occurrence without an increase in the local neural tissue astrocytic density (Sozmen et al., 2012). However, the beneficial or detrimental effects of this GFAP increase in rats submitted to MI/HF remain to be tested. The T HF rats increased GFAP-ir, but their respective control group presented similar values, which did not allow the determination of the main cause of this enhanced GFAP expression in trained animals.

It is also worth noting that MI consequences were studied after 5 weeks of the experimental procedure, a period of time relevant for the development of HF, and thus related with chronic adaptation of the nervous system to this pathological condition. Cellular numerical changes in the brain can be found as early as 1-7 days following MI (Wann et al., 2006; Kaloustian et al., 2008) and MI-induced cell death was found after 2 weeks in the whole amygdala (Bae et al., 2010). On the other hand, 2 and 3 weeks after MI, there were no apoptosis markers found in the amygdala and hippocampus of rats, although neuronal death could still be observed in the hypothalamus and prefrontal cortex (Wann et al., 2007). Because the amygdaloid complex is composed by different nuclei and subnuclei (Rasia-Filho et al., 2000; Petrovich et al., 2001; de Olmos et al., 2004), it is highly likely that differences in the sensitivity to experimental manipulations can occur on a site-specific basis. That is, within the whole amygdala, the MePD could be a putative candidate to be involved with the neuroplasticity induced by physical exercise and/or MI/HF. Our data did not support such an affirmative on the current chronic-based protocol.

Finally, some working hypotheses are opened with the present study. In this regard, further studies can be proposed to determine if different subpopulations of intrinsic neurons in the MePD (Choi et al., 2005; Carney et al., 2010) are more or less sensitive to the present experimental procedures. This would also be proposed for different GFAP-positive isoforms and the potential versatility of the GFAP cytoskeletal network (Middeldorp and Hol, 2011) and the MePD neuron-astrocyte interaction. It is also possible that differences can occur in the number of neurons and glial cells after training or MI/HF, but they have to be revealed by additional techniques that test for apoptosis or neurogenesis markers in the MePD, also checking if different compensatory ways could influence the total number of cells counted. Furthermore, it is relevant to test if the MePD of exercise-trained rats and the MePD of MI/HF animals maintain the same functional properties or if they can adapt accordingly to new allostatic conditions and alter the central sympathetic and parasympathetic modulation of the cardiovascular system. These working hypotheses require an additional methodological approach and open new possibilities for research on the structure and function of the rat MePD.

In conclusion, the present data did not evidence a modification in cellular density after preconditioning training and/or MI/HF in part of the MePD, but indicate a possible reactive gliosis and restructuring of intermediate filaments of the astrocytic cytoskeleton after MI/HF in rats.

Acknowledgements. Grants from Brazilian Agencies CNPq and CAPES. LLX and AARF are CNPq researchers.
Conflict of Interest. The authors declare no actual or potential conflict of interest.

References

Adkins D., Boychuk J., Remple M. and Kleim J. (2006). Motor training induces experience-specific patterns of plasticity across motor cortex and spinal cord. J. Appl. Physiol. 101, 1776-1782.

Bae E., Hwang I., Yoo K., Han T., Lee C., Choi J., Yi S., Lee S., Ryu P., Yoon Y. and Won M. (2010). Gliosis in the amygdala following myocardial infarction in the rat. J. Vet. Med. Sci. 72, 1041-1045.

Ben J., Soares F.M., Scherer E.B., Cechetti F., Netto C.A., Wyse A.T. (2010). Running exercise effects on spatial and avoidance tasks in ovariectomized rats. Neurobiol. Learn. Mem. 94, 312-317.

Ben J., Soares F., Cechetti F., Vuaden F., Bonan C., Netto C. and Wyse A. (2009). Exercise effects on activities of Na (+), K (+)-ATPase, acetylcholinesterase and adenine nucleotides hydrolysis in ovariectomized rats. Brain Res. 1302, 248–255.

Brusco J., Merlo S., Ikeda E.T., Petralia R.S., Kachar B., Rasia-Filho A.A. and Moreira J.E. (2014). Inhibitory and multisynaptic spines, and hemispherical synaptic specialization in the posterodorsal medial amygdala of male and female rats. J. Comp. Neurol. Dec 9. 522, 2075-2088.

Canteras S., Simerly R. and Swanson L. (1995). Organization of projections from the medial nucleus of the amygdala: a PHAL study in the rat. J. Comp. Neurol. 360, 213-245.

Carney R., Mangin J., Hayes L., Mansfield K., Sousa V., Fishell G., Machold R., Ahn S., Gallo V. and Corbin J. (2010) Sonic hedgehog expressing and responding cells generate neuronal diversity in the medial amygdala. Neural Dev. 5, 14.

Carro E., Trejo J., Busiguina S. and Torres-Aleman I. (2001). Circulating insulin-like growth factor I mediates the protective effects of physical exercise against brain insults of different etiology and anatomy. J. Neurosci. 21, 5678-5684.

Cechetti F., Rhod A., Simao F., Santin K., Salbego C., Netto C. and

Siqueira I. (2007). Effect of treadmill exercise on cell damage in rat hippocampal slices submitted to oxygen and glucose deprivation. Brain Res. 1157, 121-125.

Choi G., Dong H., Murphy A., Valenzuela D., Yancopoulos G., Swanson L. and Anderson D. (2005). Lhx6 delineates a pathway mediating innate reproductive behaviors from the amygdala to the hypothalamus. Neuron 46, 647-660.

Costa-Ferro Z., Vitola A., Pedroso M., Cunha F., Xavier L., Machado D., Soares M., Ribeiro-dos-Santos R. and DaCosta J. (2010). Prevention of seizures and reorganization of hippocampal functions by transplantation of bone marrow cells in the acute phase of experimental epilepsy. Seizure 19, 84-92.

Dall'Oglio A., Gehlen G., Achaval M. and Rasia-Filho A.A. (2008). Dendritic branching features of posterodorsal medial amygdala neurons of adult male and female rats: further data based on the Golgi method. Neurosci. Lett. 430, 151-156.

Dall'Oglio A., Xavier L., Hilbig A., Ferme D., Moreira J., Achaval M. and Rasia-Filho A. (2013). Cellular components of the human medial amygdaloid nucleus. J. Comp. Neurol. 521, 589-611.

Davern P., Jackson K.L., Nguyen-Huu T.P., La Greca L. and Head G.A. (2010). Cardiovascular reactivity and neuronal activation to stress in Schlager genetically hypertensive mice. Neuroscience 170, 551-558.

Davern P. and Head G. (2011). Role of the medial amygdala in mediating responses to aversive stimuli leading to hypertension. Clin. Exp. Pharmacol. Physiol. 38, 136-143.

Dayas C., Buller K. and Day T. (1999). Neuroendocrine responses to an emotional stressor: evidence for involvement of the medial but not the central amygdala. Eur. J. Neurosci. 11, 2312-2322.

de Castilhos J., Marcuzzo S., Forti C., Frey R., Stein D., Achaval M. and Rasia-Filho A. (2006). Further studies on the rat posterodorsal medial amygdala: dendritic spine density and effect of 8-OH-DPAT microinjection on male sexual behavior. Brain Res. Bull. 69, 131-139.

de Olmos J., Beltramino C. and Alheid G. (2004). Amygdala and extended amygdala of the rat: a cytoarchitectonical, fibroarchitectonical, and chemoarchitectonical survey. In: The rat nervous system. 3rd ed. Paxinos G. (ed). Elsevier Academic Press. San Diego. pp 509-603.

Eadie B., Redila V. and Christie B. (2005). Voluntary exercise alters the cytoarchitecture of the adult dentate gyrus by increasing cellular proliferation, dendritic complexity, and spine density. J. Comp. Neurol. 486, 39-47.

Ferraz A., Xavier L., Hernandes S., Sulzbach M., Viola G., Anselmo-Franci J., Achaval M. and Da Cunha C. (2003). Failure of estrogen to protect the substantia nigra pars compacta of female rats from lesion induced by 6-hydroxydopamine. Brain Res. 986, 200-205.

Freimann S., Scheinowitz M., Yekutieli D., Feinberg M.S., Eldar M. and Kessler-Icekson G. (2005). Prior exercise training improves the outcome of acute myocardial infarction in the rat. J. Am. Coll. Cardiol. 45, 931-938.

Gielen S., Schuler G. and Adams V. (2010). Cardiovascular effects of exercise training. Circulation 122, 1221-1238.

González-Burgos I., González-Tapia D., Zamora D., Feria-Velasco A. and Beas-Zárate C. (2011). Guided motor training induces dendritic spine plastic changes in adult rat cerebellar Purkinje cells. Neurosci. Lett. 491, 216-220.

Jaenisch R., Hentschke V., Quagliotto E., Cavinato P., Schmeing L., Xavier L. and Dal Lago P. (2011). Respiratory muscle training improves hemodynamics, autonomic function, baroreceptor sensitivity, and respiratory mechanics in rats with heart failure. J. Appl. Physiol. 111, 1664-1670.

Johnson R., Breedlove S. and Jordan C. (2008). Sex differences and laterality in astrocyte number and complexity in the adult rat medial amygdala. J. Comp. Neurol. 511, 599-609.

Jorge L., Rodrigues B., Rosa K.T., Malfitano C., Loureiro P.C.A., Medeiros A., Curi R., Brum P.C., Lacchini S., Montano N., De Angelis K. and Irigoyen M.C. (2011). Cardiac and peripheral adjustments induced by early exercise training intervention were associated with autonomic improvement in infarcted rats: role in functional capacity and mortality. Eur. Heart J. 32, 904-912.

Joyner M.J. and Green D.J. (2009). Exercise protects the cardiovascular system: effects beyond traditional risk factors. J. Physiol. 587, 5551-5558.

Kaloustian S., Wann B., Bah T., Girard S., Apostolakis A., Ishak S., Mathieu S., Ryvlin P., Godbout R. and Rousseau G. (2008). Apoptosis time course in the limbic system after myocardial infarction in the rat. Brain Res. 1216, 87-91.

Kclocke R., Tian W., Kuhlmann M. and Nikol S. (2007). Surgical animal models of heart failure related to coronary heart disease. Cardiov. Res. 74, 29–38.

Kruger L., Saporta S. and Swanson L.W. (1995). Photographic atlas of the rat brain: the cell and fiber architecture illustrated in three planes with stereotaxic coordinates. Cambridge University Press. New York. 317 pp.

Kubo T., Okatani H., Nishigori Y., Hagiwara Y., Fukumori R. and Goshima Y. (2004). Involvement of the medial amygdaloid nucleus in restraint stress-induced pressor responses in rats. Neurosci Lett. 354, 84-86.

Liu Y., Chen H., Wu C., Kuo Y., Yu L., Huang A., Wu F., Chuang J. and Jen C. (2009). Differential effects of treadmill running and wheel running on spatial or aversive learning and memory: roles of amygdalar brain-derived neurotrophic factor and synaptotagmin I. J. Physiol. 587, 3221-3231.

Longhurst J. (2008). Neural regulation of the cardiovascular system. In: Fundamental neuroscience. Squire L., Blom F., McConell S., Roberts J., Spitzer N. and Zigmond M. (eds). Academic Press. San Diego. pp 829-853.

Marcuzzo S., Dall'oglio A., Ribeiro M., Achaval M. and Rasia-Filho A. (2007). Dendritic spines in the posterodorsal medial amygdala after restraint stress and ageing in rats. Neurosci. Lett. 424, 16-21.

Martinez F., Hermel E., Xavier L., Viola G., Riboldi J., Rasia-Filho A. and Achaval M. (2006). Gonadal hormone regulation of glial fibrillary acidic protein immunoreactivity in the medial amygdala subnuclei across the estrous cycle and in castrated and treated female rats. Brain Res. 1108, 117-126.

Martins-Pinge M. (2011). Cardiovascular and autonomic modulation by the central nervous system after aerobic exercise training. Braz. J. Med. Biol. Res. 44, 848-854.

Middeldorp J. and Hol E.M. (2011). GFAP in health and disease. Prog. Neurobiol. 93, 421-443.

Morris J., Jordan C. and Breedlove S. (2008). Sexal dimorphism in neuronal number of the posterodorsal medial amygdala is independent of circulating androgens and regional volume in adult rats. J. Comp. Neurol. 506, 851-859.

Neckel H., Quagliotto E., Casali K., Montano N., Dal Lago P. and Rasia-Filho A. (2012). Glutamate and GABA in the medial amygdala induce selective central sympathetic/parasympathetic cardiovascular

responses. Can. J. Physiol. Pharmacol. 90, 525-536.

Newman S. (1999). The medial extended amygdala in male reproductive behavior. A node in the mammalian social behavior network. Ann. NY Acad. Sci. 877, 242-257.

Paxinos G. and Watson C. (2005). The rat brain in stereotaxic coordinates - The new coronal set. Elsevier. Academic Press.

Pekny M. and Pekna M. (2004). Astrocyte intermediate filaments in CNS pathologies and regeneration. J. Pathol. 204, 428-437.

Petrovich G., Canteras N. and Swanson L. (2001). Combinatorial amygdalar inputs to hippocampal domains and hypothalamic behavior systems. Brain Res. Brain Res. Rev. 38, 247-289.

Pfeffer M., Pfeffer J., Fishbein M., Fletcher P., Spadaro J., Kloner R. and Braunwald E. (1979). Myocardial infarct size and ventricular function in rats. Circ. Res. 44, 503-512.

Porter K. and Hayward L.F. (2011). Stress-induced changes in c-Fos and corticotrophin releasing hormone immunoreactivity in the amygdala of the spontaneously hypertensive rat. Behav. Brain Res. 216, 543-551.

Quagliotto E., Neckel H., Riveiro D., Casali K., Mostarda C., Irigoyen M., Dall'ago P. and Rasia-Filho A. (2008). Histamine in the posterodorsal medial amygdala modulates cardiovascular reflex responses in awake rats. Neuroscience 157, 709-719.

Quagliotto E., Casali K., Dal Lago P. and Rasia-Filho A. (2012). Neurotransmitter and neuropeptidergic modulation of cardiovascular responses evoked by the posterodorsal medial amygdala of adult male rats. In: Insights into the amygdala: Structure, functions and implications for disorders. 1st ed. Yilmazer-Hanke, D. (ed). Nova Science Publishers. Hauppauge. New York. EUA. pp 139-165.

Rasia-Filho A., Londero R. and Achaval M. (2000). Functional activities of the amygdala: an overview. J. Psychiat. Neurosci. 25, 14-23.

Rasia-Filho A., Xavier L., dos Santos P., Gehlen G. and Achaval M. (2002). Glial fibrillary acidic protein immunodetection and immunoreactivity in the anterior and posterior medial amygdala of male and female rats. Brain Res. Bull. 58, 67-75.

Rasia-Filho A., Dalpian F., Menezes I., Brusco J., Moreira J. and Cohen R. (2012a). Dendritic spines of the medial amygdala: plasticity, density, shape, and subcellular modulation by sex steroids. Histol. Histopathol. 27, 985-1011.

Rasia-Filho A., Haas D., de Oliveira A., de Castilhos J., Frey R., Stein D., Lazzari V., Back F., Pires G.N, Pavesi E., Winkelmann-Duarte E. and Giovenardi M. (2012b). Morphological and functional features of the sex steroid-responsive posterodorsal medial amygdala of adult rats. Mini Rev. Med. Chem. 12, 1090-1106.

Real C.C., Ferreira A.F.B., Chaves-Kirsten G.P., Torrão A.S., Pires R.S. and Britto L.R.G. (2013). BDNF receptor blockade hinders the benefical effects of exercise in a rat model of Parkinson's disease. Neuroscience 237, 118-129.

Rodrigues B., Figueroa D., Mostarda C., Heeren M., Irigoyen M. and De Angelis K. (2007). Maximal exercise test is a useful method for physical capacity and oxygen consumption determination in streptozotocin-diabetic rats. Cardiovasc. Diabetol. 6, 38.

Saha S. (2005). Role of the central nucleus of the amygdala in the control of blood pressure: descending pathways to medullary cardiovascular nuclei. Clin. Exp. Pharmacol. Physiol. 32, 450-456.

Saur L., Baptista P., de Senna P., Paim M., Nascimento P., Ilha J., Bagatini P., Achaval M. and Xavier L. (2014). Physical exercise increases GFAP expression and induces morphological changes in hippocampal astrocytes. Brain Struct. Funct. 219, 293-302.

Scopel D., Fochesatto C., Cimarosti H., Rabbo M., Bello-Klein A., Salbego C., Netto C. and Siqueira I. (2006). Exercise intensity influences cell injury in rat hippocampal slices exposed to oxygen and glucose deprivation. Brain Res. Bull. 71, 155-159.

Sholl D. (1953). Dendritic organization in the neurons of the visual and motor cortices of the cat. J. Anat. 87, 387-406.

Sim Y., Kim H., Kim J., Yoon S., Kim S., Chang H., Lee T., Lee H., Shin M., Shin M. and Kim C. (2005). Long-term treadmill exercise overcomes ischemia-induced apoptotic neuronal cell death in gerbils. Physiol. Behav. 84, 733-738.

Singewald N., Chicchi G.G., Thurner C.C., Tsao K-L., Spetea M., Schmidhammer H., Sreepathi H.K., Ferraguti F., Singewald G.M. and Ebner K. (2008). Modulation of basal and stress-induced amygdaloid substance P release by the potent and selective NK1 receptor antagonist L-822429. J. Neurochem. 106, 2476-2488.

Sozmen E.G., Hindman J.D. and Carmichael S.T. (2012). Models that matter: white matter stroke models. Neurotherapeutics 9, 349-358.

Stranahan A., Lee K., Becker K., Zhang Y., Maudsley S., Martin B., Cutler R. and Mattson M. (2010). Hippocampal gene expression patterns underlying the enhancement of memory by running in aged mice. Neurobiol. Aging 31, 1937–1949.

Swain R., Harris A., Wiener E., Dutka M., Morris H., Theien B., Konda S., Engberg K., Lauterbur P. and Greenough W. (2003). Prolonged exercise induces angiogenesis and increases cerebral blood volume in primary motor cortex of the rat. Neuroscience 117,1037-1046.

Tucci P. (2011). Pathophysiological characteristics of the post-myocardial infarction heart failure model in rats. Arq. Bras. Cardiol. 96, 420-424.

Turner S., Stock G. and Ganten D. (1986). Cardiovascular regulation. In: Neuroendocrinology. Lightman S. and Everitt, B. (ed). Blackwell Scientific Publications. Oxford. London. pp 331-359.

Vanoli E., Bacchini S., Panigada S., Pentimalli F. and Adamson P. (2004). Experimental models of heart failure. Eur. Heart J. (Suppl. 6), F7–F15.

Wann B., Boucher M., Kaloustian S., Nim S., Godbout R. and Rousseau G. (2006). Apoptosis detected in the amygdala following myocardial infarction in the rat. Biol. Psychiat. 59, 430-433

Wu A., Ying Z. and Gomez-Pinilla F. (2007). Omega-3 fatty acids supplementation restores mechanisms that maintain brain homeostasis in traumatic brain injury. J. Neurotrauma 24, 1587-1595.

Xavier L., Viola G., Ferraz A., Da Cunha C., Deonizio J., Netto C. and Achaval M. (2005). A simple and fast densitometric method for the analysis of tyrosine hydroxylase immunoreactivity in the substantia nigra pars compacta and in the ventral tegmental area. Brain Res. Brain Res. Protoc. 16, 58–64.

Zheng H., Li Y., Zucker I. and Patel K. (2006). Exercise training improves renal excretory responses to acute volume expansion in rats with heart failure. Am. J. Physiol. Renal Physiol. 291, F1148-1156.

Accepted May 9, 2014